# Efficient Polymer Passivation of Ligand-Stripped Nanocrystal Surfaces

**Jennifer T. Duong, Mark J. Bailey, Teresa E. Pick, Patrick M. McBride, Evelyn L. Rosen, Raffaella Buonsanti, Delia J. Milliron, Brett A. Helms**

Lawrence Berkeley National Laboratory, The Molecular Foundry, Berkeley 94720, California
Correspondence to: B. A. Helms (E-mail: bahelms@lbl.gov)

Received 27 February 2012; accepted 8 May 2012; published online
**DOI: 10.1002/pola.26178**

**ABSTRACT**: Water-dispersible, polymer-wrapped nanocrystals are highly sought after for use in biology and chemistry, from nanomedicine to catalysis. The hydrophobicity of their native ligand shell, however, is a significant barrier to their aqueous transfer as single particles. Ligand exchange with hydrophilic small molecules or, alternatively, wrapping over native ligands with amphiphilic polymers is widely employed for aqueous transfer; however, purification can be quite cumbersome. We report here a general two-step method whereby reactive stripping of native ligands is first carried out using trialkyloxonium salts to reveal a bare nanocrystal surface. This is followed by chemically directed immobilization of a hydrophilic polymer coating. Polyacrylic acids, with side-chain grafts or functional end groups, were found to be extremely versatile in this regard. The resulting polymer-wrapped nanocrystal dispersions retained much of the compact size of their bare nanocrystal precursors, highlighting the unique role of monomer side-chain functionality to serve as effective, conformal ligation motifs. As such, they are well poised for applications where tailored chemical functionality at the nanocrystal's periphery or improved access to their surfaces is desirable. © 2012 Wiley Periodicals, Inc. J Polym Sci Part A: Polym Chem 000: 000–000, 2012

**KEYWORDS**: adsorption; aqueous transfer; bare nanocrystals; biocompatibility; functional polymer coatings; interfaces; nanocomposites; nanoparticles; polymer passivation; reversible addition fragmentation chain transfer (RAFT)

**INTRODUCTION** Colloidal nanocrystals are of great interest because of their unique size and shape-dependent physical properties.[1–3] They are prepared by high-temperature synthesis routes from inorganic salts or organometallics in the presence of both coordinating and noncoordinating solvents, which serve to exert control over their size, morphology, and composition.[4,5] Once synthesized, the ligand-passivated nanocrystals are usually hydrophobic and require further manipulation before use in polar or aqueous media.[6,7] Accordingly, efficient transfer protocols for colloidal nanocrystals into water are highly desirable. This has been shown for a variety of amphiphilic polymer coatings, which leave the native coordinating ligands intact.[8–10] Although general for most nanocrystals, purification of single particles can be difficult owing to the presence of higher order supramolecular aggregates of polymers and nanocrystals. Moreover, for functional polymeric coatings, it can be difficult to assess *a priori* the optimum balance of amphiphilicity to yield the highest fraction of single particles. In cases where the physical properties of the nanocrystal are sensitive to thermal treatments in aqueous media required to anneal a tight, conformal polymer coating, the method falls short. Alternatively, native hydrophobic ligands can be displaced from the nanocrystal surface by exchanging with small molecules that contain chemical functionality directed toward metal adatoms at the nanocrystal surface.[11–16] The generality of this approach is less straightforward, as the adsorption enthalpies vary widely between various nanocrystal compositions and ligand types (anionic, dative, multivalent, etc.). In most cases, because driving the ligand exchange involves mass action,[17–24] often at high temperatures,[25–28] or nonequilibrium control via phase transfer,[29–34] the exchange efficiency is typically low. Inefficient exchange protocols may also cause undesirable nanocrystal aggregation,[35,36] in particular for biphasic procedures, and often results in irreversible adatom desorption from the nanocrystal surface or irreversible precipitation.

A more attractive approach would involve the removal of hydrophobic ligands to reveal a bare, pristine nanocrystal surface for subsequent repassivation. This has been difficult to achieve without degradation of the nanocrystal, and hence has not been previously explored. Nonetheless, dispersions of bare nanocrystals with tailored functionalities are desirable for applications in aqueous media including drug delivery,[37] bioimaging,[38,39] bioassays,[40–42] magnetic separations,[43–45] (bio)chemical remediation,[46,47] and catalysis[48,49] and also hold promise for use as nanoinks.[50–52] Toward this end, we have recently described the use of Meerwein's and

related trialkyl oxonium salts as exceptionally mild reagents that efficiently and quantitatively strip native ligands from nanocrystal surfaces without etching them or otherwise perturbing their physical properties.[53] Bare nanocrystals are likewise afforded by chemically treating nanocrystals with $NOBF_4$, although this more aggressive reagent cannot be used with Lewis-acid-sensitive metal oxides (e.g., ZnO, AZO, $Cu_2O$, etc.) or metal chalcogenides containing selenium or tellurium owing to oxidation of the chalcogenide and complete destruction of the lattice. Nevertheless, with Meerwein- or $NOBF_4$-treated nanocrystals, repassivation of the bare nanocrystal surfaces has been reported previously using small organic ligands or commercially available high-molecular-weight polyvinylpyrolidinone.[54] More deliberate passivation strategies using functional polymers especially designed to bind strongly to nanocrystal surface-bound adatoms have not yet emerged, nor has it been possible to test new coating strategies on a more complete spectrum of nanocrystal compositions, which is uniquely afforded by Meerwein's salt-based reactive ligand stripping.

Here, we show that bare nanocrystal surfaces generated using trialkyloxonium salts, with metal adatoms intact, are readily passivated by a variety of functional polymers based on the synthetically accessible polyacrylic acid (PAA) platform. The two-step strategy is highly general, and is highlighted here for dispersions of metal oxide, metal chalcogenide, and inorganic nanocrystals. The PAA scaffold is especially desirable because of the simplicity in which it can be functionalized with various end groups or side chains of differing composition or grafting density. Several new polymer coatings based on PAA are synthesized here using, for example, reversible addition fragmentation chain transfer (RAFT) polymerization[55,56] which affords excellent control over the polymer's molecular weight and polydispersity and is amenable to end-group modification.[57] The resulting polymer–nanocrystal hybrids exhibit remarkable stability over extended periods, are easy to purify, and in contrast to some previously explored methods, do not suffer from aggregation or precipitation. The protocol reported herein for preparing functional polymer–inorganic hybrid nanomaterials from bare nanocrystal dispersions dramatically simplifies their synthesis toward greater commercial scalability. Furthermore, with the ability to use a variety of polymers we can tailor the interactions of nanocrystal surfaces with biological systems to, for example, minimize toxicity thereby allowing their use in clinical setting.

## EXPERIMENTAL

### Materials and Methods

Octadecylphosphonate (ODPA)-passivated CdSe nanocrystals ($d = 4.1$ nm) and ODPA/octylamine (ODPA/OAM)-passivated CdSe/CdS quantum dot-quantum rods (QD-QRs) were prepared using an automated nanocrystal synthesis robot, WANDA, as reported by us previously.[15,58–60] Oleate passivated $\alpha$-$Fe_2O_3$ ($d = 8$ nm) were synthesized via a microwave-assisted hydrothermal route, while upconverting $\beta$-$NaYF_4$ doped with 20 mol % Yb(III) and 2 mol % Tm(III) ($d = 17$ nm) were synthesized using a high-temperature synthesis in an organic medium.[53] PAA (MW ~1800 g $mol^{-1}$) grafted with four methoxy-terminated polyethylene oxides (amide linkages) were synthesized using *N,N′*-dicyclohexylcarbodiimide (DCC)-mediated coupling.[61] All other chemicals were of the highest commercial grade possible and used as received unless otherwise stated. Monomers were distilled over $CaH_2$ prior to use. 2,2′-Azodiisobutyronitrile (AIBN) was recrystallized from ethanol. Anhydrous solvents were obtained at the highest possible purity. All buffers were prepared from biochemical grade salts and MilliQ water and sterile filtered prior to use. Automated flash chromatography was carried out on a Biotage SP1 system using HPLC-grade solvents. $^1H$ and $^{13}C$ NMR spectra were recorded in $CDCl_3$ or $CD_3OD$ using a Bruker 500 Ultrashield NMR. The solvent peak was used as a reference. IR spectra were taken using a Perkin Elmer Spectrum One Fourier transform infrared spectroscopy (FTIR) Spectrometer. Dynamic light scattering (DLS) was carried out using a Malvern Nano Series Zetasizer. Transmission electron microscopy (TEM) images were recorded on an Analytical JEOL-2100F FETEM equipped with a Gatan camera using a beam energy of 200 kV. X-ray diffraction (XRD) was performed on a Bruker Gadds-8 diffractometer with a Cu-K$\alpha$ source operating at 40 kV and 20 mA. Photoluminescence spectra and absolute quantum yields were acquired on a Horiba Jobin Yvon Fluorolog-3 Spectrofluorometer equipped with an integrating sphere.

### Synthesis of *tert*-Butyl 2-(2-(dodecylthiocarbonothioylthio)-2-methylpropanamido) ethylcarbamate Chain Transfer Agent (2)

To an ice-cold solution of 2-(dodecylthiocarbonothioylthio)-2-methylpropanoic acid **1**[62] (3.65 g, 10 mmol) in dimethylformamide (DMF) (45 mL) was added 2-(6-chloro-1H-benzotriazole-1-yl)-1,1,3,3-tetramethylaminium hexafluorophosphate (HCTU) (4.55 g, 11 mmol) portionwise, followed by *N,N*-diisopropylethylamine (DIPEA) (4.52 g, 35 mmol) in one portion and then mono Boc-protected ethylene diamine (1.60 g, 10 mmol) in DMF (5 mL). After 12 h, the reaction mixture was concentrated *in vacuo*, and the residue dissolved in diethyl ether (200 mL) prior to extraction. The ethereal layer was washed successively with saturated aqueous KCl (3 × 50 mL), saturated aqueous sodium bicarbonate (3 × 50 mL), deionized water (3 × 50 mL), and then brine (1 × 50 mL) prior to purification by flash chromatography using a gradient elution of 4:1 hexanes:DCM to 1:4. The product (**2**) was isolated as a bright yellow solid (3.30 g, 65%). $^1H$ NMR (500 MHz, $CDCl_3$): $\delta = 6.91$ (t, 1H), 4.82 (t, 1H), 3.4–3.3 (m, 6H), 1.71 (s, 6H), 1.68 (m, 2H), 1.46 (s, 9H), 1.40 (m, 2H), 1.32–1.27 (m, 16H), 0.88 (t, 3H) ppm. $^{13}C$ NMR (125 MHz, $CDCl_3$): $\delta = 173.1$, 156.4, 79.5, 57.1, 41.0, 37.1, 31.9, 29.6, 29.5, 29.4, 29.3, 29.1, 29.0, 27.7, 25.8, 22.7, 14.1 ppm. FTIR: $\nu = 3350$ (w), 2960 (s), 2927 (m), (2855) (m), 1698 (m), 1662 (m), 1528 (m), 1496 (s), 1392 (s), 1366 (m), 1278 (m), 1255(m), 1175 (m), 1146 (m), and 815 (m) $cm^{-1}$. Anal. Calcd for ($C_{24}H_{46}N_2O_3S_3$): C, 56.87; H, 9.15; N, 5.53; S, 18.98. Found: C, 56.84; H, 9.20; N, 5.51; S, 18.93.

### Synthesis of Boc-NH-$CH_2CH_2$-Poly(*tert*-Butyl Acrylate)-Trithiocarbonate (3)

A solution containing chain transfer agent (CTA) **2** (253 mg, 0.50 mmol), *tert*-butyl acrylate (1.60 g, 12.5 mmol), and AIBN (8.0 mg, 0.05 mmol) was charged into a 50-mL Schlenk tube and degassed using four cycles of a freeze–pump–thaw sequence. The polymerization was then carried out at 70°C for 1 h. The polymer was precipitated three times in 1:3 MeOH:$H_2O$ from acetone, and the residue dissolved in DCM before drying over anhydrous $MgSO_4$, filtering and concentrating to give the final polymer (**3**) as a viscous yellow product (1.40 g, 76%). Monomer conversion was determined to be ~80% by $^1$H NMR. $^1$H NMR (500 MHz, $CDCl_3$): $\delta$ = 3.4–3.2 (m, 4H), 2.3–2.1 (m, 30H) 1.9–0.7 (m, 380H) ppm. FTIR: $\nu$ = 2979 (m), 2936 (m), 2894 (s), 1729 (m), 1529 (s), 1482 (s), 1458 (m), 1373 (m), 1368 (m), 1355 (s), 1152 (m), 1044 (s), 925 (s), 847 (m), and 755 (s) $cm^{-1}$. Anal. Calcd for ($C_{164}H_{286}N_2O_{43}S_3$): C, 64.16; H, 9.39; N, 0.91; S, 3.13. Found: C, 64.10; H, 9.50; N, 0.92; S, 3.08. THF-SEC: $M_n$ =2750 g $mol^{-1}$; $M_w$ = 2840 g $mol^{-1}$; PDI = 1.03.

### Synthesis of $H_2N$-$CH_2CH_2$-Poly(acrylic acid)-Trithiocarbonate (4)

Polymer **3** (1.0 g, mmol) was dissolved in DCM (10 mL) prior to the addition of an equivolume of trifluoroacetic acid (TFA). The reaction mixture was stirred for 24 h before concentrating *in vacuo* to yield the final product (**4**) as a yellow foam (615 mg, 100%). $^1$H NMR (500 MHz, MeOD): $\delta$ = 2.5–2.3 (s, 32H), 2.0–0.9 (m, 72H) ppm. FT-IR: $\nu$ = 3500(m), 3120 (m), 2941 (m), 2878 (s), 2600 (m), 1716 (m), 1457 (m), 1264 (m), 1207 (m), and 820 (s) $cm^{-1}$. Anal. Calcd for ($C_{79}H_{118}N_2O_{41}S_3$): C, 51.35; H, 6.44; N, 1.52; S, 5.21. Found: C, 51.30; H, 6.48; N, 1.53; S, 5.14.

### Synthesis of FITC-NH-$CH_2$-$CH_2$-Poly(acrylic acid)-Trithiocarbonate (5)

Polymer **4** (92 mg, 0.05 mmol) was dissolved in 50 mM borate buffer at pH 9.0 (2 mL) (and the pH adjusted with 5 N NaOH until a pH of 9.0 was achieved) and the solution cooled in an ice bath prior to the addition of fluorescein isothiocyanate (96 mg, 0.25 mmol) as an aliquot in dry DMSO (300 μL). The reaction was placed on a rotating carousel in a cold room maintained at 4°C for 6 h before passing through a PD10 Size Exclusion Column (GE Healthcare) equilibrated to MilliQ water to remove unreacted dye. The fraction containing FITC-labeled polymer was acidified with 1 N HCl until a pH of 2–3 was obtained prior to lyophilization. The crude product **5** (i.e., containing some residual NaCl salts) was isolated as a yellow–orange solid and used without further purification. $^1$H NMR (500 MHz, MeOD): $\delta$ = 8.1–6.5 (m, 9H), 2.4–2.3 (s, 39H) 2.0–0.9 (m, 94H) ppm. FTIR: $\nu$ = 3475 (m) 2956 (m), 2596 (s), 1724 (m), 1457 (s), 1424 (s), 1267 (m), and 828 (s) $cm^{-1}$. Anal. Calcd for ($C_{100}H_{129}N_3O_{46}S_4$): C, 53.68; H, 5.81; N, 1.88; S, 5.73. Found: 50.75; H, 5.25; N, 1.80; S, 5.36. The deviation in the elemental analysis from the calculated is consistent with the incomplete reprotonation of all of the sodium acrylates following the work-up. On average, this is ~6 Na acrylates per polymer. The solubility of **5**, compared to pristine PAA was also noted—where some portion of water (up to 10% w/w) was preferred when attempting to dissolve into polar aprotic solvents like DMF for the NC passivation.

### Preparation of Bare Nanocrystal Dispersions in DMF

Ligand stripping reactions were performed in a nitrogen drybox. Equal volumes of nanocrystals in hexanes (1–20 mg $mL^{-1}$) and Meerwein's salt or, alternatively, $Me_3OBF_4$ dissolved in acetonitrile (ACN) (1–10 mM) containing DMF (0–10 eq. with respect to the trialkylammonium salt) were combined, resulting in a biphasic solution. Upon gentle agitation, a precipitate consisting of bare nanocrystals was observed. Chloroform (2 mL) was added to the reaction and the bare nanocrystals were pelleted by centrifugation at 2500 RPM for 1–3 min (Eppendorf Centrifuge 5702). The supernatant was discarded and the pellet was washed with additional chloroform (4 mL) and pelleted (2×) before redispersing in DMF (1 mL). The resulting dispersions were transparent and stable for months. In the case of QD-QRs, the preferred method involved direct transfer to DMF containing $Me_3OBF_4$ (10 mM). Quenching of the excess alkylating agent, if necessary, could be carried out via addition of *N,N*-diisopropyl-2-ethanolamine. Here, the alcohol serves as a sacrificial nucleophile, whereas the internal nonnucleophilic, tertiary amine serves to quantitatively neutralize the *in situ*-formed $HBF_4$ upon alkylation of the alcohol.

### Preparation of Polymer-Wrapped Nanocrystals

A dispersion of bare nanocrystals in DMF (25–100 μL) was added to 1 mL of DMF containing the PAA-derived polymer coating of interest (10 mg $mL^{-1}$). An additional volume of water was required to dissolve PAA-FITC into DMF, most likely owing to the presence of residual salt. In all cases, then, the reaction mixture was sonicated for 1–2 h before adding dropwise into 50 mM borate buffer at pH 9 (20 mL). After stirring (30 min or 24 h, depending on the sample), the solution was purified and concentrated to a final volume ~1 mL via spin dialysis (MWCO = 10, 30, or 50 kDa depending on the size of the nanocrystal and molecular weight of the polymer coating, Millipore Amicon Ultra).

### Preparation of Citrate-Passivated Nanocrystals

A similar procedure was carried out for the passivation by small molecules. In this case, citric acid in DMF (up to 100 mg $mL^{-1}$) was employed.

## RESULTS AND DISCUSSION

The use of trialkyloxonium salts to rapidly and efficiently remove native hydrophobic ligands leaves the nanocrystal surface bare, with cationic metal adatoms residing at their surfaces along with anions (e.g., $BF_4^-$) weakly interacting electrostatically in their place [Scheme 1(a)].

We have shown in previous study that these stripped nanocrystals can be redispersed in polar solvents that engage in dative coordination to their cationic adatoms (e.g., DMF or HMPA).[53] Indeed, FTIR of dried nanocrystal films—either CdSe, CdSe/CdS, $\alpha$-$Fe_2O_3$, or upconverting $\beta$-$NaYF_4$:Yb/Tm-treated first with $Me_3OBF_4$ in ACN, precipitated, and redispersed in DMF showed characteristic stretches in the

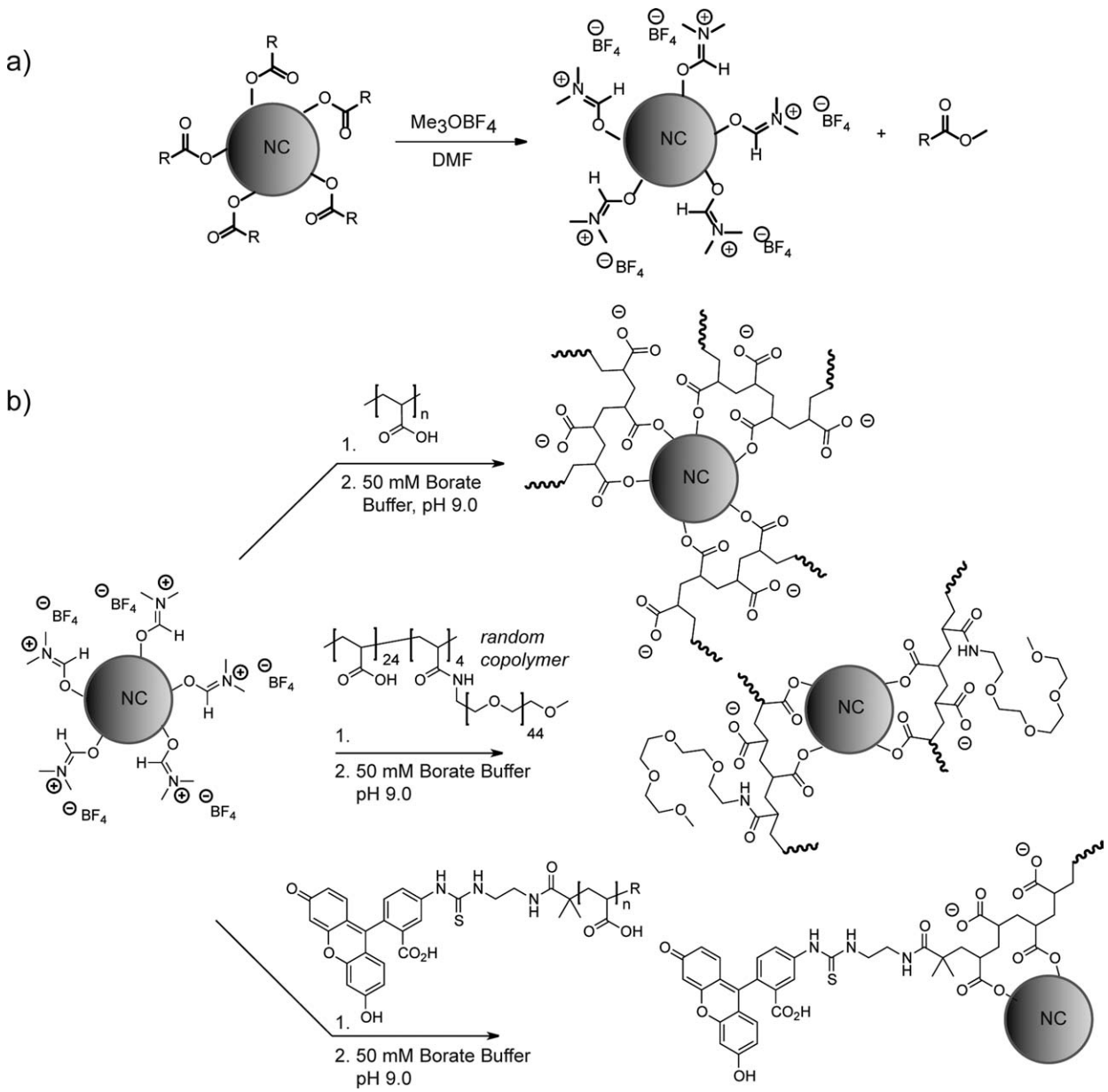


**SCHEME 1** (a) Reactive ligand stripping of nanocrystals using trimethyloxonium tetrafluoroborate and redispersion in DMF: NC = $\alpha$-$Fe_2O_3$, CdSe, $\beta$-$NaYF_4$:Yb/Tm, or CdSe/CdS QD-QRs. (b) Passivation of bare NCs surfaces with poly(acrylic acid)-derived polymers (e.g., PAA, PAA-m$PEO_4$, PAA-FITC) and subsequent transfer into aqueous buffers.

carbonyl region consistent with DMF-adsorbates to surface adatoms. No etching of the nanocrystals was observed by TEM (Fig. 1).

This dynamic, dative coordination sphere of DMF ligands is shown here to be readily displaced in favor of stronger-coordinating anionic carboxylate functionality present on polymer side chains [Scheme 1(b)]. PAA was selected as a platform for passivating nanocrystals with functional polymers both on the basis of its coordination potential to adatoms at the nanocrystal surface, as well as its straightforward synthesis from commercially available materials or via controlled radical polymerization. In addition to low-molecular-weight PAA polymer adsorbates, a series of functional polymer coatings were prepared to assess the generality of the method. For example, PAA grafted with 2000 Da methoxy-terminated polyethylene oxides[63–66] (PAA-m$PEO_4$) was useful for preparing nanocrystals with PEGylated peripheries. Additionally, we prepared a fluorescein-terminated PAA using RAFT polymerization, following the sequence shown in Scheme 2.

Briefly, a nascent amino-modified RAFT CTA **2** was prepared from Boc-ethylene diamine and the trithiocarbonate CTA **1** using HCTU in DMF in the presence of DIPEA. The polymerization of *tert*-butyl acrylate was then carried out using CTA

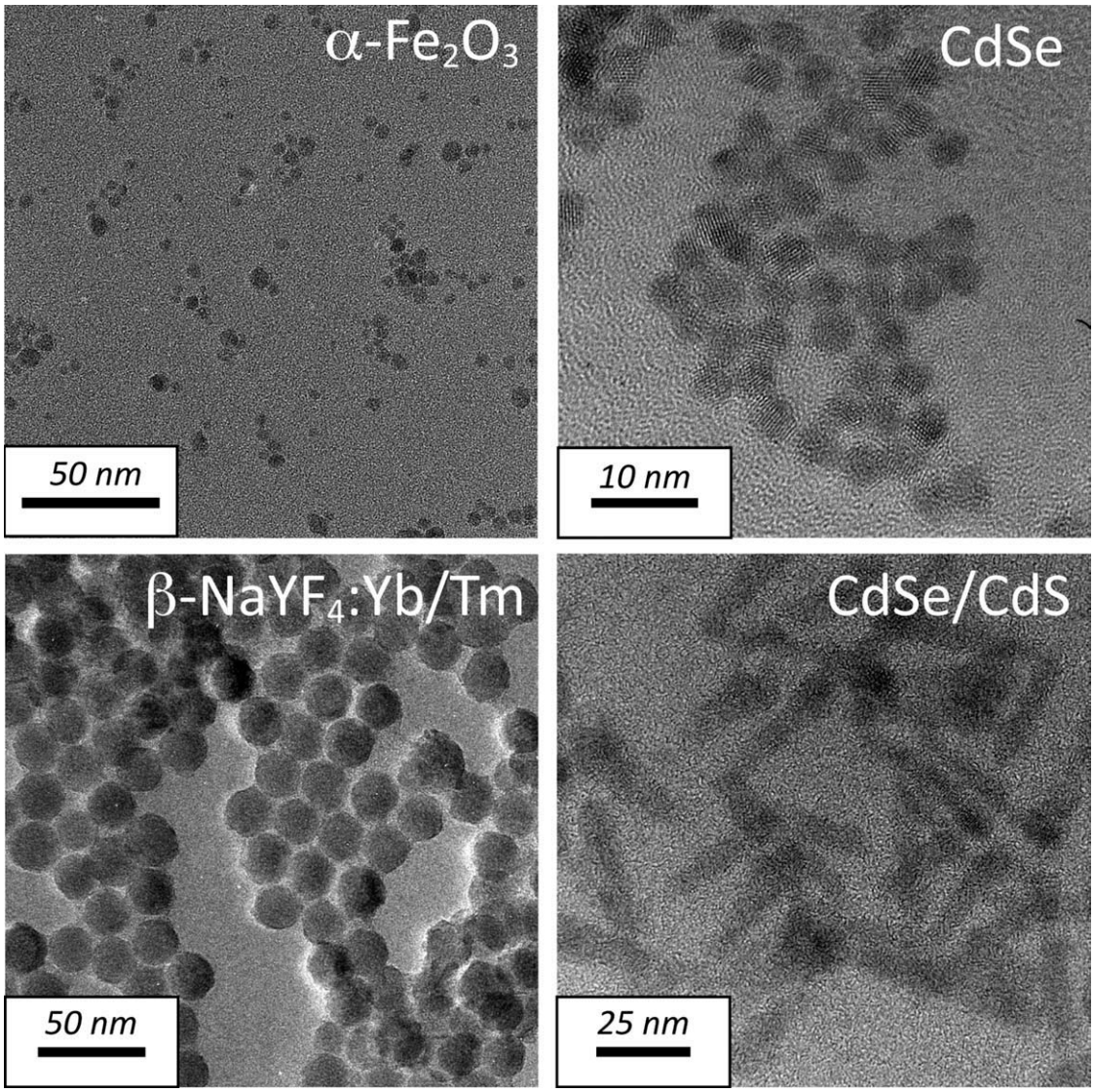


**FIGURE 1** Transmission electron micrographs of ligand stripped, bare nanocrystals: $\alpha$-$Fe_2O_3$, CdSe, $\beta$-$NaYF_4$:Yb/Tm and CdSe/CdS QD-QRs. The removal of native ligands is concomitant with nanocrystal clustering.

**2** in the presence of AIBN, where [tBu Acrylate]:[**2**]:[AIBN] was 25:1:0.1. The monomer conversion was ~80% after 1 h at 70°C. The RAFT process afforded a narrowly dispersed product (PDI = 1.03), where the observed number average molecular weight was determined to be $M_n = 2750$ g mol$^{-1}$ and the weight average was $M_w = 2840$ g mol$^{-1}$. The Boc-terminus and side-chain *tert*-butyl groups were quantitatively deprotected using TFA in DCM (24 h) prior to labeling the amine chain end with FITC (50 mM borate buffer, pH 9.0, 6 h). To verify the robustness of a polymer passivation approach for coating bare nanocrystals over a small molecule with a similar coordination motif, citrate was also investigated.

The rapid attachment of PAA-derived polymers to bare nanocrystal surfaces was accomplished by combining polymers dissolved in DMF (10 mg mL$^{-1}$) to DMF dispersions of bare nanocrystals (25–100 μL). The resulting dispersions were sonicated briefly and then transferred dropwise into basic aqueous buffer (50 mM borate buffer, pH 9.0). Polymer-wrapped nanocrystals were readily purified by spin dialysis. In that all of the polymer coatings used here were low molecular weight and did not self-assemble into supramolecular aggregates, the purification of excess materials from the wrapped nanocrystals was significantly improved (i.e., did not require extensive purification by size exclusion chromatography, as is a standard practice to yield single nanocrystals). These dispersions were significantly more stable (i.e., no precipitation) than those with citrate as a ligand; unequivocal precipitation occurred for citrate-coated nanocrystals within a few hours post-aqueous transfer (Fig. 2). Furthermore, control experiments where, for example, oleate-passivated $\alpha$-$Fe_2O_3$ nanocrystals were allowed to exchange their surface passivation with PAA-m$PEO_4$ at room temperature and in THF did not produce aqueous dispersible

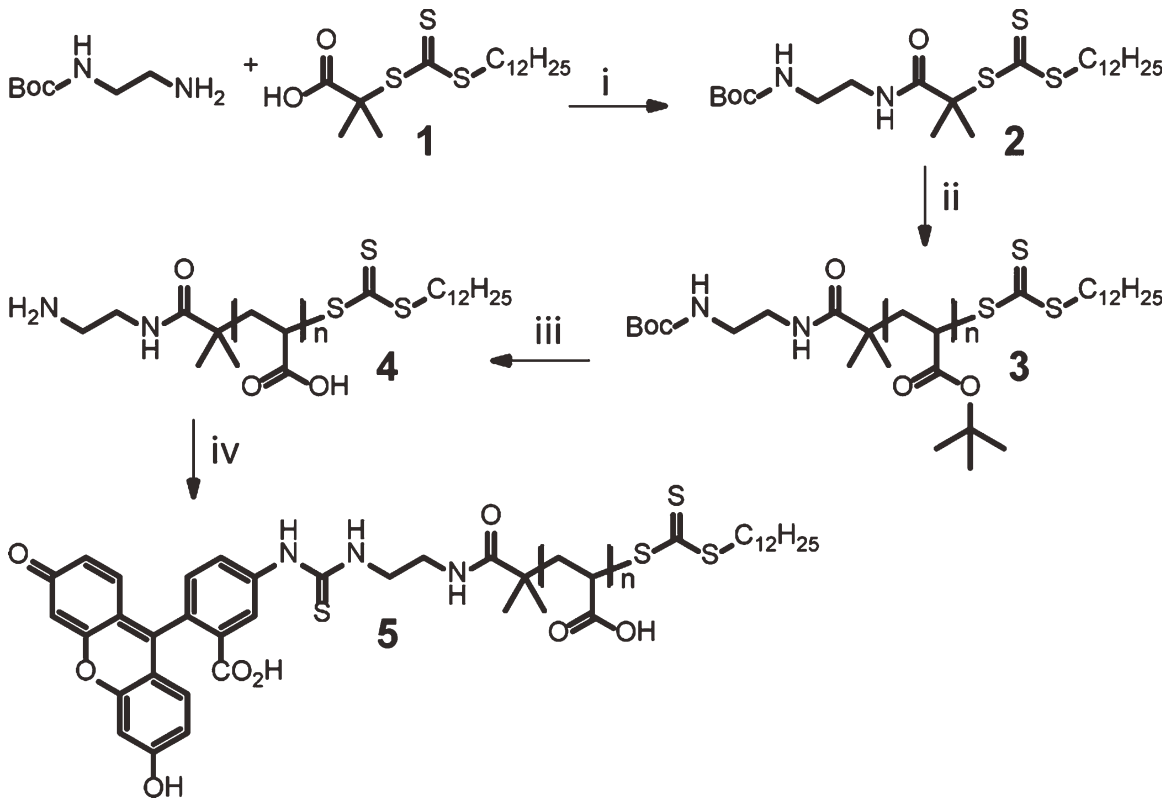


**SCHEME 2** Chemical synthesis of a FITC-terminated PAA for passivating the surfaces of bare nanocrystals. Reagents: (i) HCTU, DIPEA, DMF; (ii) tBu-Acrylate, AIBN; (iii) DCM, TFA; (iv) FITC, borate buffer, pH 9.0.

materials, highlighting the importance of first stripping the hydrophobic native ligands prior to passivation with functional PAA-based coatings.

To verify the size distribution and quality of the wrapping procedure, DLS was used to measure the hydrodynamic diameters of both bare nanocrystals dispersed in DMF as well as their wrapped counterparts. Nanocrystals passivated with unmodified PAA coatings exhibited the smallest size increase relative to the bare nanocrystal precursor. For example, $\alpha$-$Fe_2O_3$ nanocrystals initially ~7–8 nm in diameter, once wrapped with PAA, gave a hydrodynamic diameter of 9 nm. In contrast, for coatings based on PAA-mPEO$_4$, a hydrodynamic diameter of 12 nm was observed. The larger size associated with the PAA-mPEO$_4$ wrapping can be attributed to the polyethylene oxide grafts extending from the nanocrystal surface. For $\alpha$-$Fe_2O_3$ passivated with citrate, however, a hydrodynamic diameter of 33 nm indicated significant aggregation even at this early stage of repassivation. The robustness of the polymer passivated approach was confirmed by images of $\alpha$-$Fe_2O_3$ nanocrystals succeeding aqueous transfer. Those nanocrystals possessing the PAA-derived polymer coat were nonaggregated, exhibiting stable uniform dispersions and an overall retention of nanocrystal quality. In contrast, the citrate wrapping of $\alpha$-$Fe_2O_3$ was inefficient, resulting in aggregation of nanocrystals [Fig. 2(a)].

A similar trend was delineated for the wrapping of bare, upconverting $NaYF_4$:Yb/Tm. In this case, similar hydrodynamic diameters ~18–20 nm were observed for both the PAA and the PAA-mPEO$_4$-wrapped nanocrystals, where the bare nanocrystals were ~17 nm. For citrate-capped nanocrystals, however, the diameter was measured at 28 nm consistent with significant aggregation using this procedure. Metal chalcogenide nanocrystals were also efficiently transferred to water with direct binding of metal adatoms to polymer-bound carboxylates. Thus, for 4.1 nm CdSe nanocrystals, hydrodynamic diameters of 6 and 9 nm for CdSe wrapped with PAA and PAA-mPEO$_4$, respectively, were observed. CdSe nanocrystals passivated by PAA-derived polymers exhibited nonaggregated, uniform dispersions over extended periods of time [Fig. 2(b)]. By contrast, a citrate coating was so poor at stabilizing dispersions of CdSe that the sample resulted in precipitation shortly after the aqueous transfer; the hydrodynamic diameter was, therefore, not measurable.

This strategy was also successful in manipulating the surface of nanocrystals with more elaborate polymer coatings. For example, FITC-PAA polymer **5** derived from RAFT polymerization was readily placed at the surface of otherwise colorless dispersions of bare, upconverting $NaYF_4$:Yb/Tm nanocrystals. Upconverting nanocrystals based on these materials offer photostable luminescence ideal for single particle imaging, sharp emission bandwidths, and large anti-Stokes shifts. Previously reported syntheses of aqueous dispersible, upconverting nanocrystals typically require heating for extended periods of time to displace native coordinating ligands with

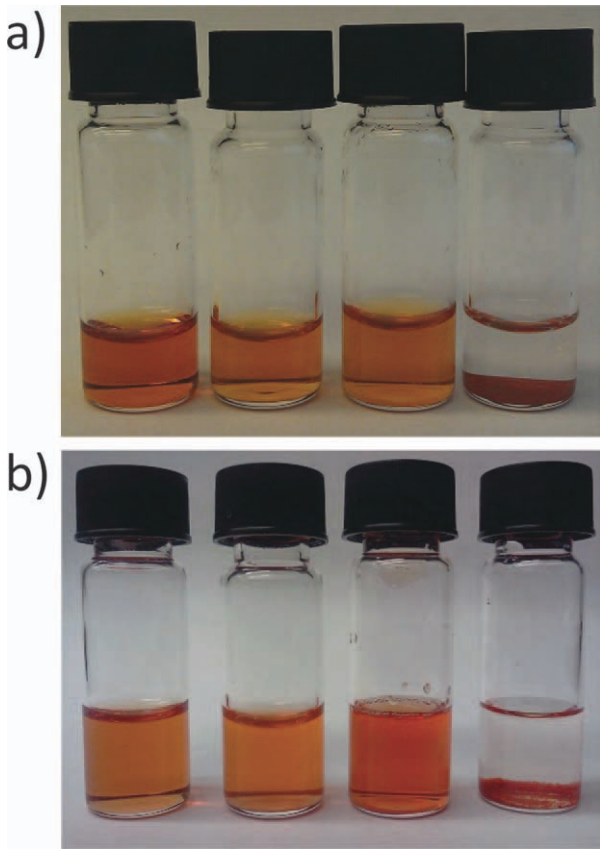


**FIGURE 2** (a) Aqueous dispersions of repassivated $\alpha$-$Fe_2O_3$ nanocrystals: PAA, PAA-mPEO$_4$, PAA-FITC, or citrate-coated nanocrystals (left to right); (b) Aqueous dispersions of repassivated CdSe nanocrystals: PAA, PAA-mPEO$_4$, PAA-FITC, citrate-coated nanocrystals (left to right).

polymeric ligands. This process is known to slowly degrade the lattice over time at the high temperatures required for exchange.[67] Loss of ions from the nanocrystal lattice both reduces the number of sensitizing/emitting species and affects phonon coupling and energy transfer efficiency in the nanocrystal owing to differences in interfacial strain for particles of different sizes. This is completely avoided using the strategy reported here. The mildness of our two-step procedure was able to retain both the luminescence of the appended dyes now localized to the nanocrystal surface as well as dimensions and crystal phase of the $NaYF_4$ lattice that is necessary to maintain high-photon upconversion efficiency. The FITC dye was readily detected both in the presence and in the absence of UV light, tinting colorless $NaYF_4$:Yb/Tm with a readily observable yellow hue [Fig. 3(a, b)].

The dispersions were uniform and stable (i.e., no precipitation). The XRD pattern of $NaYF_4$:Yb/Tm showed the expected highly emissive $\beta$-phase and its power-dependent emission profile upon excitation at $\lambda_{ex} = 980$ nm was taken to confirm its crystal structure and upconverted luminescence [Fig. 3(c, d)]. Chromogenic tags for these otherwise colorless nanocrystals may also be useful in performing further manipulations (e.g., labeling with proteins or other biomolecules) using standard purification and detection apparatus found in most laboratories engaged in synthetic chemistry or chemical biology.

We were also interested in characterizing the limitations, if any, of using a PAA-platform as a stabilization strategy for luminescent metal chalcogenide nanocrystals, in particular as these have not been explored previously. To that end, we investigated in detail the effects on the photophysical properties upon sequential manipulation of CdSe/CdS QD-QRs surfaces, from their native ligand coordination sphere of ODPA and OAM to stripping and repassivation with either

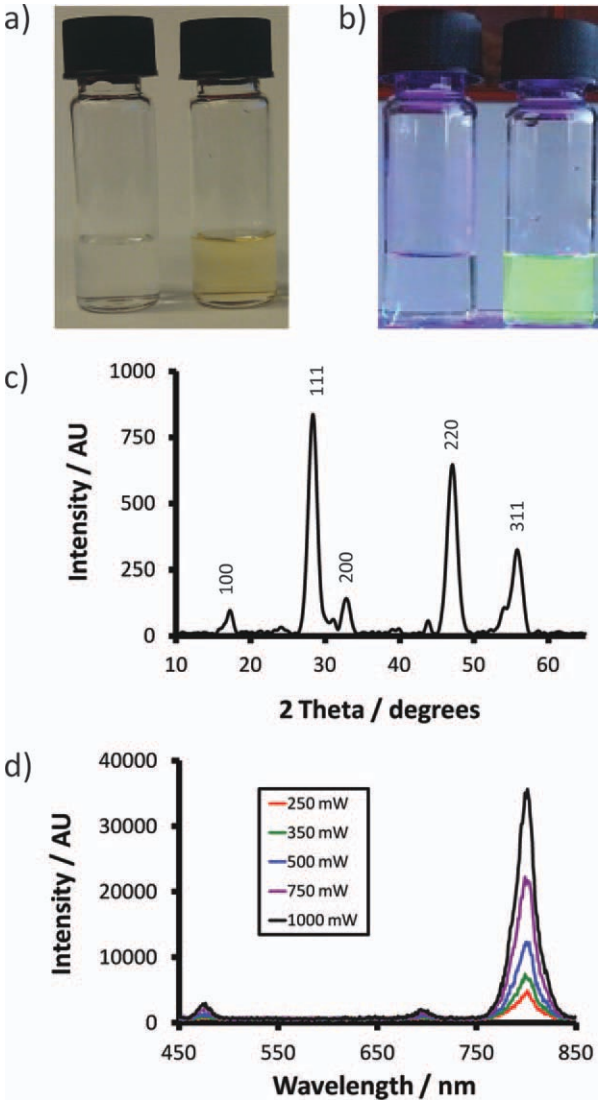


**FIGURE 3** Characterization of polymer passivated upconverting nanocrystals: (a) aqueous dispersions of $\beta$-$NaYF_4$:Yb/Tm nanocrystals passivated by PAA-FITC in ambient light; (b) aqueous dispersions of $\beta$-$NaYF_4$:Yb/Tm upconverting nanocrystals passivated by PAA-FITC illuminated from below with UV light; (c) X-ray diffraction pattern of $\beta$-$NaYF_4$:Yb/Tm nanocrystals showing characteristic peaks for the highly emissive hexagonal phase; (d) Power-dependent upconverted emission from $\beta$-$NaYF_4$:Yb/Tm excited at $\lambda_{ex} = 980$ nm.

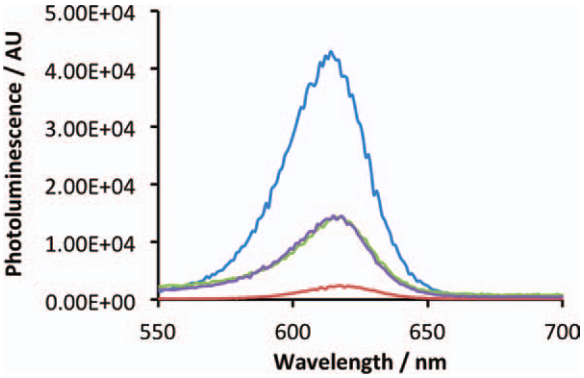


**FIGURE 4** Photoluminescence spectra of CdSe/CdS quantum dot-quantum rod nanocrystal heterostructures at the same optical density: ODPA/OAM coated (blue), ligand stripped (red), PAA coated (green), and PAA-mPEO$_4$ coated (purple).

PAA or PAA-mPEO$_4$ (Fig. 4). The QD-QRs initially had a photoluminescence quantum yield (PLQY) of 43%, measured in hexanes using a fluorometer equipped with an integrating sphere. The emission maximum was $\lambda_{em} = 614$ nm. Upon stripping and dispersing into DMF, the PLQY decreased to ~2.4% and the emission maximum red-shifted to $\lambda_{em} = 620$ nm. The emission at longer wavelengths for stripped QD-QRs confirms that reactive ligand stripping is exceptionally mild (i.e., does not etch, which would shift the emission to shorter wavelengths owing to confinement effects[68]) and also suggests that the presence of DMF at dative coordination sites at the nanocrystal surface has the effect of modulating the energetics of the exciton's relaxation, most likely owing to effects on the nanocrystal's phonon modes. As with the CdSe nanocrystals, repassivation was successfully realized for both PAA and PAA-mPEO$_4$. QD-QRs wrapped with either of these coatings shared nearly identical photophysics: both had PLQY values between 14 and 15%, thus recovering favorably from the losses incurred upon stripping, and both had an emission maximum at $\lambda_{em} = 617$ nm. These data collectively suggest that recovery of photoluminescence to ~33% of the original QD-QRs with their native ligands intact is directly related to carboxylate vs. DMF binding at the nanocrystal surface. The extent of photoluminescence recovery is also similar to that observed for the displacement of native ligands by small molecules.[69] Thus, we can infer that the extent to which PAA-derived macromolecules are able to conform and passivate trap sites at the nanocrystal surface is competitive with that for small-molecule ligands. In that, grafting additional functionality along the PAA backbone, in this case mPEO chains, does not adversely affect this recovery points more generally to opportunities in future schemes to deliberately engineer the topological display of different chemical functionalities using these coatings. PAA-derived coatings should offer a more reliable platform in that regard than might otherwise be carried out using, for example, amphiphilic polymers where functionalization can be upset in the balance of amphiphilicity required to efficiently wrap the nanocrystal and also to ensure its aqueous solubility as required for purification.

## CONCLUSIONS

We have developed a general, two-step strategy for generating polymer-wrapped nanocrystals from dispersions of bare nanocrystals and hydrophilic polymers. Metal oxide, metal chalcogenide, and inorganic nanocrystals and heterostructures are amenable to repassivation, as shown here, with PAA-based polymer ligands for use in aqueous media. The method is exceptionally mild, minimizing damage to nanocrystals surfaces, and was observed to provide a more robust coating long term compared to small molecules like citrate. In carrying out this approach, the use of amphiphilic polymers is completely avoided, which dramatically simplifies the purification of the hybrids. As colloidal dispersions, these new aqueous nanocrystal compositions remained stable for months. Our approach should broadly apply to other functional polymer coatings specifically tailored for biological and chemical applications.

## ACKNOWLEDGMENTS

Emory Chan is thanked for synthesizing the CdSe/CdS QD-QRs using the Foundry's automated nanocrystal synthesis robot, WANDA. Virginia Altoe is also thanked for helpful discussions and TEM of the stripped QD-QRs. All work was carried out at the Molecular Foundry and was supported by the Director, Office of Science, Office of Basic Energy Sciences, Division of Materials Sciences and Engineering, of the US Department of Energy under Contract No. DE-AC02-05CH11231. These materials are available for collaborative research through the Molecular Foundry's User Program (foundry.lbl.gov).

## REFERENCES AND NOTES

**1** Alivisatos, A. P. *Science* **1996,** *271*, 993–937.

**2** Alivisatos, A. P. *J. Phys. Chem. C* **1996,** *100*, 13226–13239.

**3** Yin, Y.; Alivisatos, A. P. *Science* **2005,** *437*, 664.

**4** Jun, Y. W.; Choi, J. S.; Cheon, J. *Angew. Chem. Int. Ed.* **2006,** *45*, 3414–3439.

**5** Laurent, S.; Forge, D.; Port, M.; Roch, A.; Robic, C.; Elst, L. V.; Muller, R. N. *Chem. Rev.* **2008,** *108*, 2064–2110.

**6** Park, J.; Joo, J.; Kwan, S. G.; Jang, Y.; Hyeon. T. *Angew. Chem. Int. Ed.* **2007,** *46*, 4630–4660.

**7** Murray, C. B.; Norris, D. J.; Bawendi, M. G. *J. Am. Chem. Soc.* **1993,** *115*, 8706–8715.

**8** Pellegrino, T.; Manna, L.; Kudera, S.; Liedl, T.; Koktysh, D.; Rogach, A. L.; Keller, S.; Radler, J.; Natile, G.; Parak, W. J. *Nano Lett.* **2004,** *4*, 703–707.

**9** Petruska, M. A.; Bartko, A. P.; Klimov, V. I. *J. Am. Chem. Soc.* **2004,** *126*, 714–715.

**10** Lees, E. E.; Nguyen, T.-L.; Clayton, A. H. *A.; Mulvaney, P. ACS Nano* **2009,** *3*, 1121–1128.

**11** Zhang, T.; Ge, J.; Hu, Y.; Yin, Y. *Nano Lett.* **2007,** *7*, 3203–3207.

**12** Gittins, D. I.; Caruso, F. *Angew. Chem. Int. Ed.* **2001,** *40*, 3001–3004.

**13** De Palma, R.; Peeters, S.; Van Bael, M. J.; Van den Rul, H.; Bonroy, K.; Laureyn, W.; Mullens, J.; Borghs, G.; Maes, G. *Chem. Mater.* **2007,** *19*, 1821–1831.

**14** Mei, B. C.; Susumu, K.; Medintz, I.; Mattoussi, H. *Nat. Protoc.* **2009,** *4*, 412–423.

**15** Caldwell, M. A.; Albers, A. E.; Levy, S. C.; Pick, T. E.; Cohen, B. E.; Helms, B. A.; Milliron, D. J. *Chem. Commun.* **2011,** *47*, 556–558.

**16** Llordes, A.; Hammack, A. T.; Buonsanti, R.; Tangirala, R.; Aloni, S.; Helms, B. A.; Milliron, D. J. *J. Mater. Chem.* **2011,** *21*, 11631–11638.

**17** Gaponik, N.; Talapin, D. V.; Rogach, A. L.; Eychmuller, A.; Weller, H. *Nano Lett.* **2002,** *2*, 803–806.

**18** Dubois, F.; Mahler, B.; Dubertret, B.; Doris, E.; Mioskowski, C. J. *Am. Chem. Soc.* **2007,** *129*, 482–483.

**19** Mitchell, G. P.; Mirkin, C. A.; Letsinger, R. L. *J. Am. Chem. Soc.* **1999,** *121*, 8122–8123.

**20** Mattoussi, H.; Mauro, J. M.; Goldman, E. R.; Anderson, G. P.; Sundar, V. C.; Mikulec, F. V.; Bawendi, M. G. *J. Am. Chem. Soc.* **2000,** *122*, 12142–12150.

**21** Chan, W. C. W.; Nie, S. *Science* **1998,** *281*, 2016–2018.

**22** Hermanson, G. T. Bioconjugate Techniques; Academic Press: San Diego, **2008.**

**23** Talapin, D. V.; Murray, C. B. *Science* **2005,** *310*, 86–89.

**24** Kovalenko, M. V.; Scheele, M.; Talapin, D. V. *Science* **2009,** *324*, 1417–1420.

**25** Millstone, J. E.; Hurst, S. J.; Metraux, S. G.; Cutler, J. I.; Mirkin, C. A. *Small* **2009,** *5*, 646–664.

**26** Lokteva, I.; Radychev, N.; Witt, F.; Borchert, H.; Parisi, J.; Kolyny-Olesiak, J. J. *Phys. Chem. C* **2010,** *114*, 12784–12791.

**27** Peng, X.; Schlamp, M. C.; Kadavanich, A. V.; Alivisatos, A. P. *J. Am. Chem. Soc.* **1997,** *119*, 7019–7029.

**28** Wang, Y.; Zeiri, O.; Neyman, A.; Stellacci, F.; Weinstock, I. A. *ACS Nano* **2012,** *6*, 629–640.

**29** Liu, D.; Snee, P. T. *ACS Nano* **2011,** *5*, 546–550.

**30** Yu, W. W.; Chang, E.; Sayes, C. M.; Drezek, R.; Colvin, V. L. *Nanotechnology* **2006,** *17*, 4483–4487.

**31** Pong, B.-K.; Trout, B. L.; Lee, J.-Y. *Langmuir* **2008,** *24*, 5270–5276.

**32** Jiang, W.; Mardyani, S.; Fischer, H.; Chan, W. C. W. *Chem. Mater.* **2006,** *18*, 872–878.

**33** Smith, A. M.; Duan, H.; Rhyner, M. N.; Ruan, G.; Nie, S. *Phys. Chem. Chem. Phys.* **2006,** *8*, 3895–3903.

**34** Aldana, J.; Wang, Y. A.; Peng, X. *J. Am. Chem. Soc.* **2001,** *123*, 8844–8850.

**35** Potapova, I.; Mruk, R.; Zentel, R.; Basche, T.; Mews, A. *J. Am. Chem. Soc.* **2003,** *125*, 320–321.

**36** Andala, D. M.; Shin, S. H. R.; Lee, H.-Y.; Bishop, K. J. M. *ACS Nano* **2012,** *6*, 1044–1050.

**37** Kim, J.; Kim, H.-S.; Lee, N.; Kim, T.; Kim, H.; Yu, T.; Song, I.-C.; Moon, W.-K.; Hyeon, T. *Angew. Chem. Int. Ed.* **2008,** *47*, 8438–8441.

**38** Liu, G. L.; Yin, Y. D.; Kunchakarra, S.; Mukherjee, B.; Gerion, D.; Jett, S. D.; Bear, D. G.; Gray, J. W.; Alivisatos, A. P.; Lee, L. P.; Chen, F. Q. F. *Nat. Nanotechnol.* **2006,** *1*, 47–52.

**39** Norris, D. J.; Efros, A. L.; Erwin, S. C. *Science* **2008,** *319*, 1776–1779.

**40** Mattoussi, H.; Mauro, J. M.; Goldman, E. R.; Anderson, G. P.; Sundar, V. C.; Mikulec, F. V.; Bawendi, M. G. *J. Am. Chem. Soc.* **2000,** *122*, 12142–12150.

**41** Han, M.; Gao, X.; Su, J. Z.; Nie, S. *Nat. Biotechnol.* **2001,** *19*, 631–635.

**42** Zhao, X.; Hilliard, L. R.; Mechery, S. J.; Wang, Y.; Bagwe, R. P.; Jin, S.; Tan, W. *Proc. Natl. Acad. Sci. USA* **2004,** *101*, 15027–15032.

**43** Yavuz, C. T.; Mayo, J. T.; Yu, W. M.; Prakash, A.; Falkner, J. C.; Yean, S.; Cong, L.; Shipley, H. J.; Kan, A.; Tomson, M.; Natelson, D.; Colvin, V. *Science* **2006,** *314*, 964–967.

**44** Probst, C. E.; Zrazhevskiy, P.; Gao, X. *J. Am. Chem. Soc.* **2011,** *133*, 17126–17129.

**45** Yang, H.; Qu, L.; Wimbrow, A. N.; Jiang, X.; Sun, Y. *Int. J. Food Microbiol.* **2007,** *118*, 132–138.

**46** Dagan, G.; Sampath, S.; Lev, O. *Chem. Mat.* **1995,** *7*, 446–453.

**47** Nagappa, B.; Chandrappa, G. T. *Micropor. Mesopor. Mat.* **2007,** *106*, 212–218.

**48** Stowell, C. A.; Korgel, B. A. *Nano Lett.* **2005,** *5*, 1203–1207.

**49** Mondloch, J. E.; Wang, Q.; Frenkel, A. I.; Finke, R. G. *J. Am. Chem. Soc.* **2010,** *132*, 9701–9714.

**50** Dasgupta, S.; Kruk, R.; Mechau, N.; Hahn, H. *ACS Nano* **2011,** *5*, 9628–9638.

**51** Okamura, K.; Mechau, N.; Nikolova, D.; Hahn, H. J. *Mater. Chem.* **2010,** *20*, 5651–5658.

**52** Kim, H.-S.; Dhage, S. R.; Shim, D.-E.; Hahn, H. T. *Appl. Phys. A Mater.* **2009,** *97*, 791–798.

**53** Rosen, E. L.; Buonsanti, R.; Llordes, A.; Sawvel, A. M.; Milliron, D. J.; Helms, B. A. *Angew. Chem. Int. Ed.* **2012,** *51*, 684–689.

**54** Dong, A.; Ye, X.; Chen, J.; Kang, Y.; Gordon, T.; Kikkawa, J. M.; Murray, C. B.; *J. Am. Chem. Soc.* **2011,** *133*, 998–1006.

**55** Chiefari, J.; Chong, Y. K.; Ercole, F.; Krstina, J.; Jeffery, J.; Le, T. P. T.; Mayadunne, R. T. A.; Meijs, G. F.; Moad, C. L.; Moad, G.; Rizzardo, E.; Thang, S. H. *Macromolecules* **1998,** *31*, 5559–5562.

**56** Loiseau, J.; Doeerr, N.; Suau, J. M.; Egraz, J. B.; Llauro, M. F.; Ladaviere, C.; Claverie, J. *Macromolecules* **2003,** *36*, 3066–3077.

**57** Llauro, M-F.; Loiseau, J.; Boisson, F.; Delolme, F.; Ladaviere, C.; Claverie, J. *J. Polym. Sci. A Polym. Chem.* **2004,** *42*, 5439–5462.

**58** Albers, A. E.; Chan, E. M.; McBride, P. M.; Ajo-Franklin, C. M.; Cohen, B. E.; Helms, B. A. *J. Am. Chem. Soc. Submitted for publication.*

**59** Carbone, L.; Nobile, C.; De Giorgi, M.; Della Salla, F.; Morello, G.; Pompa, P.; Hytch, M.; Snoeck, E.; Fiore, A.; Franchini, I. R.; Nadasan, M.; Silvestre, A. F.; Chiodo, L.; Kudera, S.; Cingolani, R.; Krahne, R.; Manna, L. *Nano Lett.* **2007,** *7*, 2942–2950.

**60** Talapin, D. V.; Rogach, A. L.; Kornowski, A.; Haase, M.; Weller, H.; *Nano Lett. 2001, 1, 207–211.*

**61** Bailey, M. J.; van der Weegen, R.; Klemm, P. J.; Baker, S. L.; Helms, B. A. *Adv. Healthcare Mater.* **2012** (doi: 10.1002/adhm.2012 00039).

**62** Lai, J. T.; Filla, D.; Shea, R. *Macromolecules* **2002,** *35*, 6754–6756.

**63** Na, B. H.; Palui, G.; Rosenberg, J. T.; Ji, X.; Grant, S. C.; Mattoussi, H. *ACS Nano* **2012,** *6*, 389–399.

**64** Walkey, C. D.; Olsen, J. B.; Guo, H.; Emili, A.; Chan, W. C. W. *J. Am. Chem. Soc.* **2012,** *134*, 2139–2147.

**65** Song, H.-T.; Choi, J.-S.; Huh, Y.-M.; Kim, S.; Jun, Y.-W.; Suh, J.-S.; Cheon, J. *J. Am. Chem. Soc.* **2005,** *127*, 9992–9993.

**66** Harris, J. M. *J. Macromol. Sci. C Polym. Rev.* **1985,** *25*, 325–373.

**67** Naccache, R.; Vetrone, F.; Mahalingam, V.; Cuccia, L. A.; Capobianco, J. A. *Chem. Mater.* **2009,** *21*, 717–723.

**68** Lin, W.; Fritz, K.; Guerin, G.; Bardajee, G. R.; Hinds, S.; Sukhovatkin, V.; Sargent, E. H.; Scholes, G. D.; Winnik, M. A. *Langmuir* **2008,** *24*, 8215–8219.

**69** Caldwell, M. A.; Albers, A. E.; Levy, S. C.; Pick, T. E.; Cohen, B. E.; Helms, B. A.; Milliron, D. J. *Chem. Commun.* **2011,** *47*, 556–558.